

Asymmetric Lasercom for Small Unmanned Aerial Systems

P.G. Goetz,¹ W.T. Freeman,² J.L. Murphy,¹ B. Mathieu,³ S.J. Frawley,² M.R. Suite,⁴ M.S. Ferraro,¹ W.R. Smith,⁴ B.B. Xu,⁴ R. Mahon,¹ W.S. Rabinovich,¹ M.A. Colbert,² H.R. Burris,⁴ C.I. Moore,⁴ and W.W. Schultz⁵

¹Optical Sciences Division

²SmartLogic

³Barry Design, LLC

⁴Naval Center for Space Technology

⁵Chemistry Division

Introduction: As reliance on small unmanned aerial systems (UASs) expands, and sensors requiring higher-bandwidth downlinks are developed, the need for secure high-data-rate communications increases. Laser communication (lasercom), also known as free-space optical (FSO) communication, is inherently low-probability-of-interception and detection (LPI/LPD). Lasercom has been previously demonstrated on manned aircraft; however, those systems require a high-precision pointing system and correspondingly high-accuracy navigation information hardware, both of which are prohibitively heavy for small UASs.

The work described here opens up the use of lasercom to small UASs, which could not otherwise support lasercom terminals. NRL developed an alternative to conventional lasercom terminals and applied it to small UASs. The enabling technology in these new terminals is the modulating retro-reflector (MRR). NRL has actively developed MRRs since 1998, primarily for terrestrial and shipboard applications. An MRR architecture shifts most of the power, weight, and pointing requirements to one end of the link, allowing the other end to be extremely small, low-power, and require only rough pointing.

Airborne Lasercom Transceiver Components: NRL's MRR transmitters and photoreceivers require only coarse pointing ($\pm 15^\circ$). An optical amplitude modulator is mounted in the path of a cornercube retro-reflector. The ground station's laser beam is

retro-reflected back with data impressed on the beam. MRR transmitters and photoreceivers are installed in modified, low-cost, lightweight (65 g) camera gimbals to allow hemispherical coverage.

Dakota Wingpod Lasercom System: The MRR transceiver gimbals, stabilized camera, and electronics are installed in a wingpod. Hardware providing GPS position, inertial sensing, and heading are included. An onboard processor maintains pointing to the laser ground station. An RF modem in the tail of one pod adds the capability to make hardware configuration changes while in flight for testing purposes. The final weights of the pods are 3.6 kg and 3.1 kg, including gimballed lasercom transmitter and receiver, stabilized camera, video compressor/modem, navigation data sources, antennas, pod structure, and mounting hardware. The combined power draws and weights of the components required for communication are 6 W and 1 kg, and can readily be further reduced. The pods require only power and an optional GPS antenna feed from the Dakota. Figure 1 shows the Dakota with wingpods.

Lasercom Ground Station: The lasercom ground station is based on the Dual Mode Optical Interrogator (DMOI) developed by NovaSol and NRL under the Office of Naval Research DMOI program. NRL extended the capabilities of the DMOI to allow it



FIGURE 1
Dakota UAS with MRR lasercom wingpods.

to track aircraft. Using GPS information, a gimbal provides coarse pointing, putting the aircraft into the field of view of the DMOI's fine steering mirrors, which then optically track the lasercom transceiver. The DMOI is 305 mm by 254 mm by 279 mm, requires



FIGURE 2
Dual Mode Optical Interrogator (DMOI) on tripod.

FIGURE 3
Frame captured from a 15 frames/second video stream.



100 to 180 W, and is controlled by a laptop. The laser system has been classified ANSI / IEC Class 1M, which is eye-safe out of the aperture. Figure 2 shows the DMOI on a tripod.

Flight Tests: NRL successfully completed flight tests on a Dakota UAS at Dugway Proving Ground, Utah, from June 15 to 19, 2009. Two pods were carried on the Dakota. The pods operated independently, allowing various configurations to be tested on the same flight. Maximum range was 2.5 km. The data rate on all links was 2 Mb/s. Three types of links were demonstrated:

- 1) Live video was captured on the ground using the lasercom downlink, while pointing and zoom commands were sent to the camera via the lasercom uplink. A frame captured from a 15 frames/second video stream is shown in Fig. 3.
- 2) Video was stored onboard while the aircraft was out of range, followed by download of the video files over the lasercom link when it came back in range.

- 3) An Ethernet link was established and used for two-way file transfer and communication with the aircraft.

Current and Future Work: The information gained from the flight tests is being used to develop more advanced airborne lasercom payloads. Work is currently under way to increase range while decreasing size and weight for use on expendable, long-range UASs for intelligence, surveillance, and reconnaissance (ISR).

Acknowledgments: The authors would like to thank Matt Sinfield, Jason Wooden, Mark Nielson, and Amy Secrist of the Space Dynamics Lab for assisting with integrating the wingpods and operating the Dakota, Dave Stuart for piloting the Dakota, and Yevgeniya (Jane) Case of L3 Geneva Aerospace for operating the Dakota autopilot.

[Sponsored by the OSD Rapid Reaction Technology Office]

Reference

¹ W.S. Rabinovich, R. Mahon, H.R. Burris, G.C. Gilbreath, P.G. Goetz, C.I. Moore, M.F. Stell, M.J. Vilcheck, J.L. Witkowski, L. Swingen, M.R. Suite, E. Oh, and J. Koplow, "Free-space Optical Communications Link at 1550 nm Using Multiple-Quantum-Well Modulating Retroreflectors in a Marine Environment," *Optical Engineering* 44(5), 056001(2005).

SWOrRD: Swept-Wavelength Optical resonance-Raman Detection of Bacteria, Chemicals, and Explosives

J. Grun,¹ C. Manka,² P. Kunapareddy,² R. Lunsford,² D. Gillis,³ S. Nikitin,² Z. Wang,⁴ J. Bowles,³ and M. Corson³

¹*Plasma Physics Division*

²*RSI Inc.*

³*Remote Sensing Division*

⁴*Center for Bio/Molecular Science and Engineering*

Introduction: Detection of bacteria, chemicals, or explosives with Raman scattering is fast, noncontact, does not require chemical supplies, and is adaptable to robotic vehicles — making Raman ideal for many military and civilian applications. In this technique, a laser is used to illuminate an area that may contain the sought-after substance. Some of the laser light is absorbed by the molecular vibrational and rotational states of the substance, and is re-emitted (scattered) at wavelengths slightly different than the wavelength of the illuminating laser. The spectrum of this scattered light is unique to the substance's molecular bond structure, forming a signature that can be used for identification. However, the fraction of laser light that is Raman scattered is very small, leading to insufficient sensitivity in many practical situations. Furthermore, the illuminated area may contain many different substances, each scattering its own Raman spectrum. What is measured is the sum of these spectra, which can be quite complex, so that the ability to identify the constituent substances (i.e., the method's specificity) is degraded. There remains a continuing need to improve the specificity and sensitivity of Raman detection.

When the photon energy of the illuminating laser matches one or more of the energies of the substance's vibrational and rotational states, the laser is said to be in resonance with the substance, and the scattering process is called resonance-Raman. In resonance, the amount of absorbed laser light is significantly greater, and so is the amount of scattered light: light scattered through resonance-Raman is 100 to 100,000 times more intense than light scattered through a Raman process. Thus, we expect that resonance-Raman detection would result in a much better sensitivity (~ ppm

for Raman in ideal environments), or equivalently, allow much larger distance from which detection can be made. However, this is hard to realize in practice. Current detectors use lasers operating at a single laser wavelength, which are not necessarily in resonance with the bonds of the sought-after substance, or are resonant with bonds of one substance but not with those of another.

Swept-Wavelength Optical resonance-Raman

Detection: The potential for increased sensitivity of resonance-Raman can be achieved if a way is found to illuminate the sample with more than one wavelength, chosen to be resonant with the substance's rotational and vibrational states. And, as discussed below, illuminating with more than one wavelength adds another important capability — increased selectivity in complex environments, i.e., environments that contain many different substances.

We are developing two technologies to enable practical multiwavelength resonance-Raman detection.^{1,2,3} The first technology is SWOrRD, Swept-Wavelength Optical resonance-Raman Detection, a multiwavelength resonance-Raman system that sequentially illuminates an area with a laser tunable from deep-ultraviolet to near-infrared and acquires resonance-Raman spectra at each illumination wavelength with a two-stage tunable spectrometer. All components of the SWOrRD system are synchronized, under computer control, and switching wavelengths takes less than one second. The laser has certain unique characteristics that make it especially suitable for detection: narrow bandwidth, low peak power, and high average power (see Fig.4).

A comparison of a multiwavelength resonance-Raman signature of the explosive HMX and a resonance-Raman signature of HMX acquired by illuminating with a single wavelength is shown in Fig. 5. Looking at the single illumination wavelength signature, it is easy to imagine how the distinctive features of this signature are lost once noise and the signatures of other substances are superimposed on it, resulting in a loss of specificity. The multiwavelength signature is composed of multiple spectra, each produced by illumination with a distinct laser wavelength, which are assembled to form a 2D signature, the two independent dimensions being laser-illumination wavelength and scattered wave numbers. In addition to the information contained in the single spectrum, this 2D signature contains information reflecting variations in resonance cross sections with illumination wavelength. It is therefore much more robust and harder to confuse, resulting in better specificity, especially in complex environments containing many different substances.

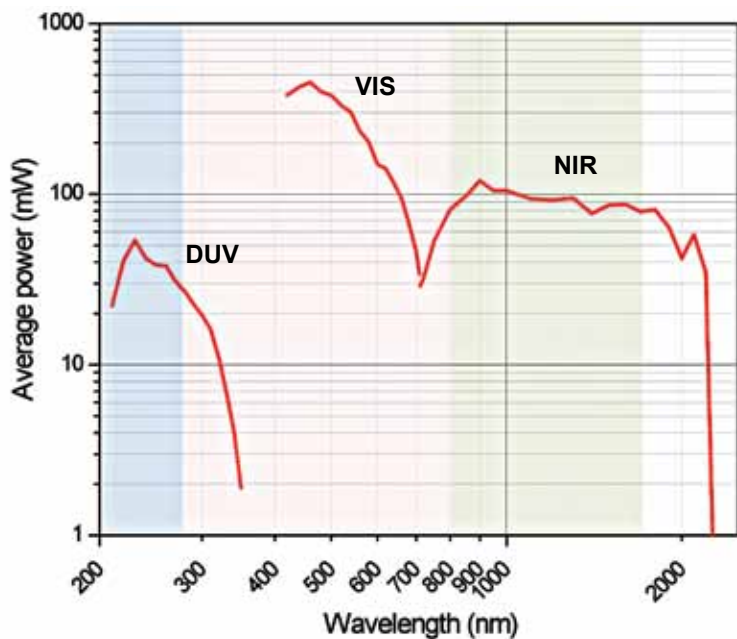
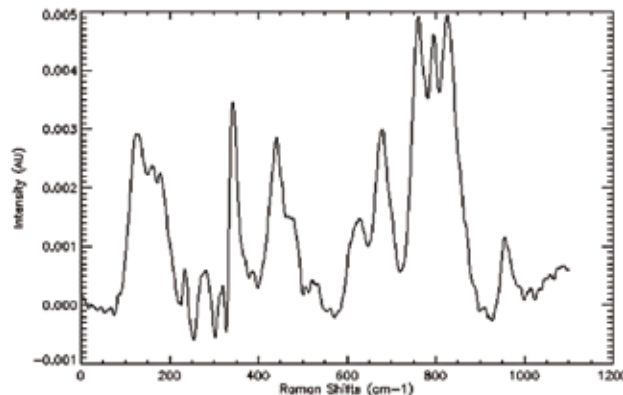
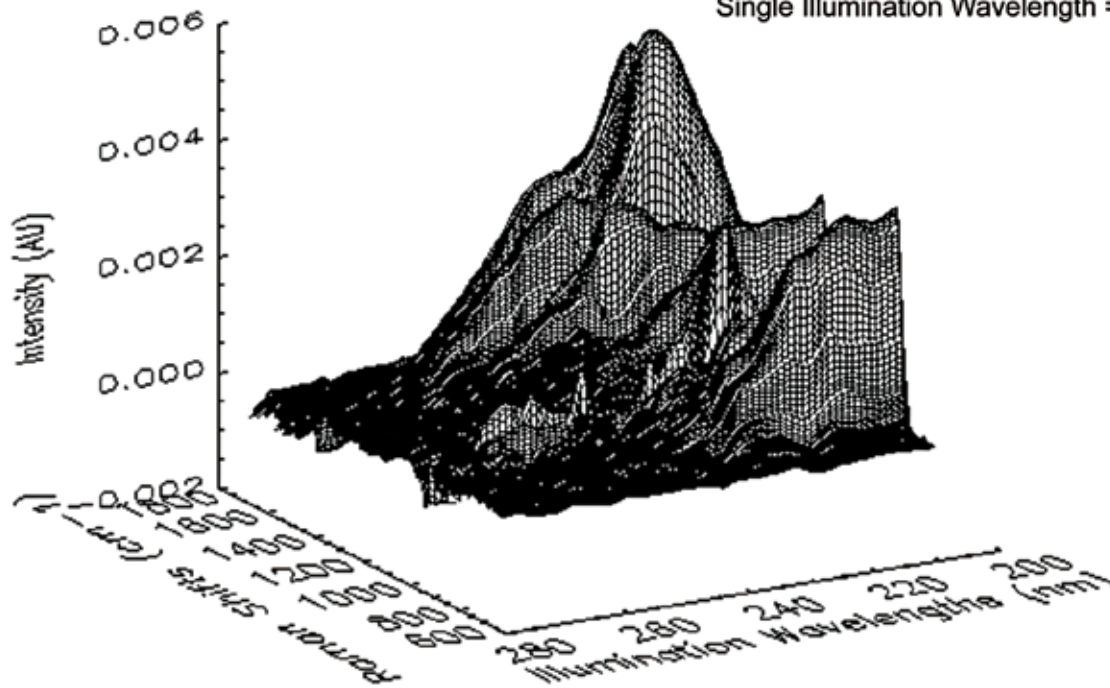


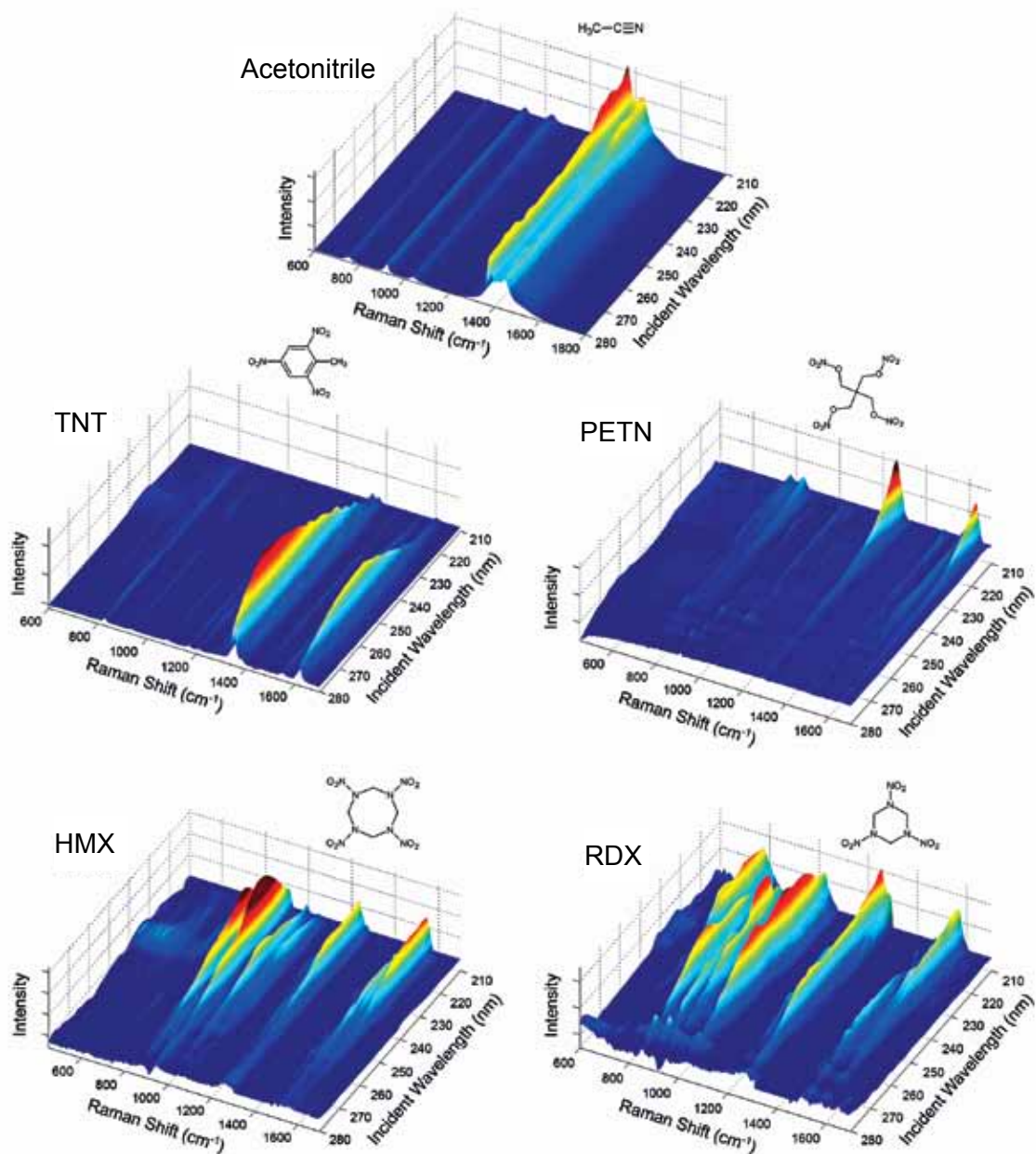
FIGURE 4
Average laser power of the SWOrD laser as a function of wavelength. The laser runs at 1 kHz, has a line width of about 4 cm^{-1} , and is tunable in less than 1 s in 0.1-nm steps.

FIGURE 5
One- and two-dimensional resonance-Raman spectra of the explosive HMX. Top right: A spectrum acquired by illumination with 261-nm laser light. Bottom left: A spectrum acquired by illuminating with multiple laser wavelengths from 210 to 270 nm.



Single Illumination Wavelength = 261 nm



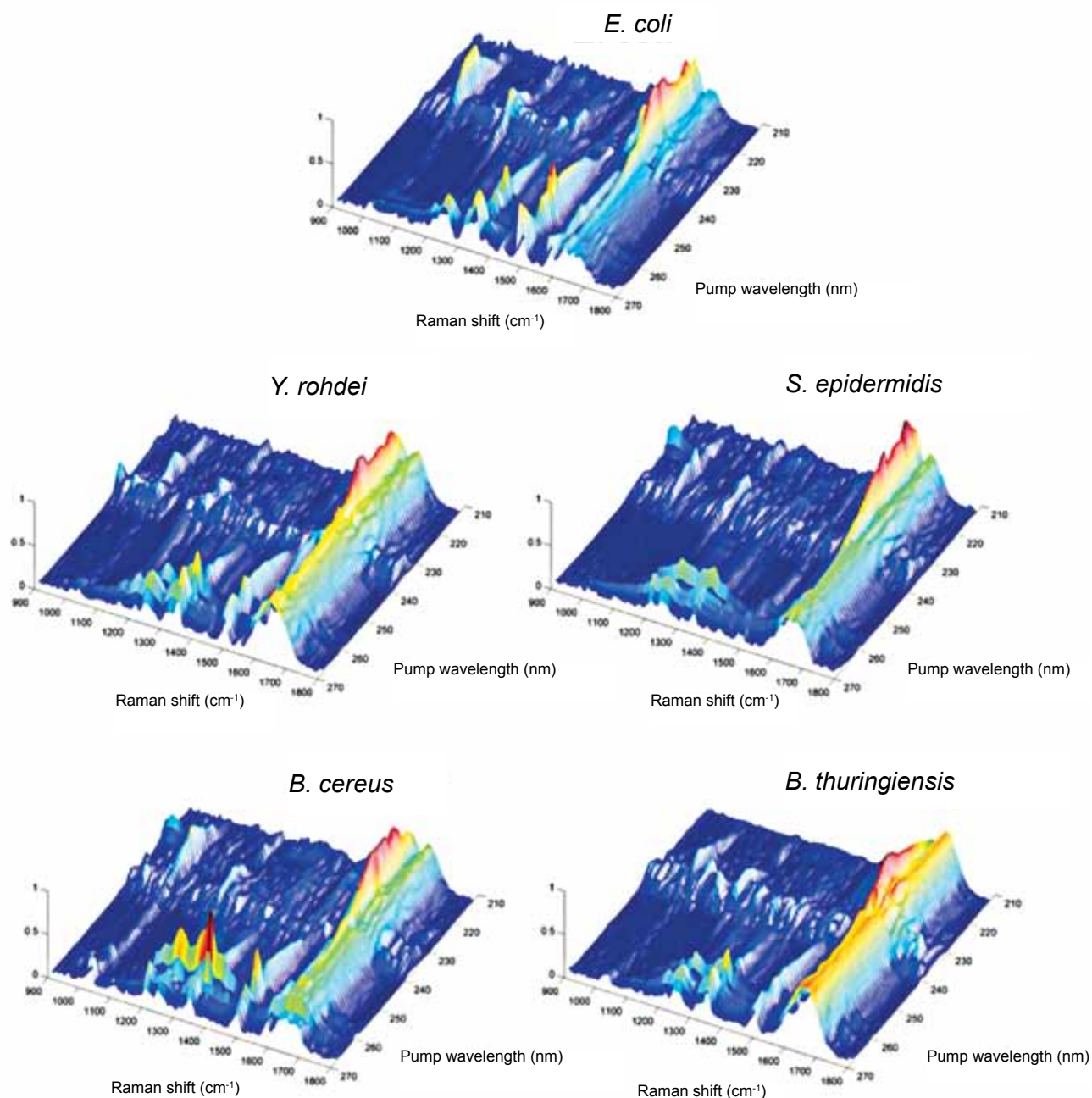
**FIGURE 6**

Two-dimensional spectral signatures of acetoneitrile, TNT, PETN, HMX, and RDX. The horizontal axes are the resonance-Raman shift wavenumbers and the illumination wavelengths, and the vertical axes are spectrum intensities.

Figure 6 shows the 2D signatures of a few explosives, and Fig. 7 shows 2D signatures of selected bacteria.

The second technology we are developing is a set of algorithms that will enable automated identification of substances from their 2D resonance-Raman signatures, even when the substances sought after are mixed with many other substances, i.e., when they are present in a complex environment. The algorithms are based on ORASIS, the Optical Real-time Adaptive Spectral Identification System,⁴ a class of algorithms based on the linear mixture model that was originally developed for analysis of satellite and aerial

hyperspectral imagery, where it was used to identify objects in complex scenes that contained many objects in addition to the one being sought. ORASIS will be adapted to SWOrRD detection because the application is similar, namely, identifying the spectral signature of a particular substance within a spectrum originating from many different substances. The algorithms are used as follows. First, 2D signatures of pure substances are measured and stored in a digital library. A signature measured in the field, and assumed to be a linear combination of some of the signatures that are stored in the library, is introduced to the code. In a process analogous to an inverse Fourier transform, the code

**FIGURE 7**

Bacterial signatures. Two-dimensional resonance-Raman signatures of *E. coli*, *Y. rohdei*, *S. epidermidis*, *B. cereus*, and *B. thuringiensis*.

determines which library signatures make up the field-measured signature, and thus identifies the chemical present and the amount.

Conclusion: We are currently working on developing SWOrRD technology to the point where it is practical to field, and are also adopting it for medical applications. Two-dimensional signatures of bacteria, explosives, chemicals used to manufacture explosives, pharmaceuticals, and assorted chemicals that may occur in the environment are being measured. The

ORASIS code is being adopted so it can take a measured signature of a complex mixture and decompose it into constituent signatures, such as those shown in Figs. 6 and 7.

[Sponsored by DTRA]

References

- ¹ J. Grun, C.K. Manka, S. Nikitin, D. Zabetakis, G. Comanescu, D. Gillis, and J. Bowles, "Identification of Bacteria from Two-Dimensional Resonant-Raman Spectra," *Analytical Chemistry* 79(14), 5489–5493 (2007).

- ² G. Comanescu, C.K. Manka, J. Grun, S. Nikitin, and D. Zabetakis, "Identification of Explosives with Two-Dimensional Ultraviolet Resonance Raman Spectroscopy," *Applied Spectroscopy* **62**, 833–839 (2008).
- ³ S. Nikitin, C. Manka, and J. Grun, "Modified Solc Notch Filter for Deep Ultraviolet Applications," *Appl. Opt.* **48**(6), 1184–1189 (2009).
- ⁴ J. Bowles, P. Palmadesso, J. Antoniadis, M. Baumbach, and L.J. Rickard, "Use of Filter Vectors in Hyperspectral Data Analysis," *Proc. SPIE* **2553**, 148–157 (1995).

Single-shot Imaging Magnetometry and Spectroscopy Using Cold Atoms

F.K. Fatemi,¹ M.L. Terraciano,¹ M. Bashkansky,¹ and Z. Dutton²

¹*Optical Sciences Division*

²*Radar Division and BBN Technologies*

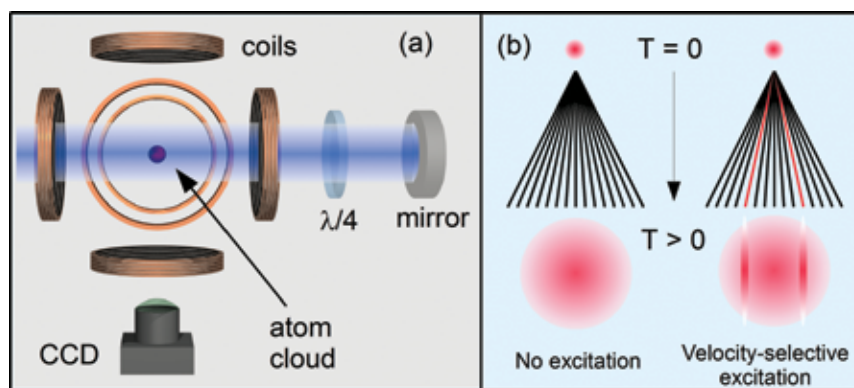
Introduction: Ultracold ($T \sim 100$ microKelvin) atoms are promising candidates for next-generation inertial sensors and magnetometers, but there are several technical challenges to optimizing their performance. The atoms must be initiated efficiently into specific electronic states, and good knowledge and control of magnetic fields is required. To address these issues, we have developed a simple, single-shot technique for imaging ambient magnetic fields with submillimeter spatial resolution over a few centimeters, and for simultaneous measurement of the atomic internal state distribution. This allows real-time optimization of experimental parameters. Such diagnostics previously required time-consuming measurements that prevented real-time evaluation. Our technique requires no hardware beyond what is already used in a typical cold atom setup.

Background: A typical cold atom trap [Fig. 8(a)] confines approximately 10^7 rubidium atoms in a 1 mm diameter volume. When the atoms are released, the cloud freely expands with a distribution of velocities [Fig. 8(b)]. At a later time, the atoms have dispersed spatially according to their velocities so that a fluorescence image of the expanded cloud represents the velocity distribution: under normal conditions, this expanded cloud has a smooth Gaussian profile. In our technique, we can selectively excite atoms within a narrow velocity class because the excitation laser frequency is Doppler-shifted into resonance only for specific velocities. Resonant velocity-selected atoms show up in the image as increased fluorescence [Fig. 8(b), right]. The associated Doppler shifts are proportional to the external fields, and can be used to measure the populations of magnetic sublevels.

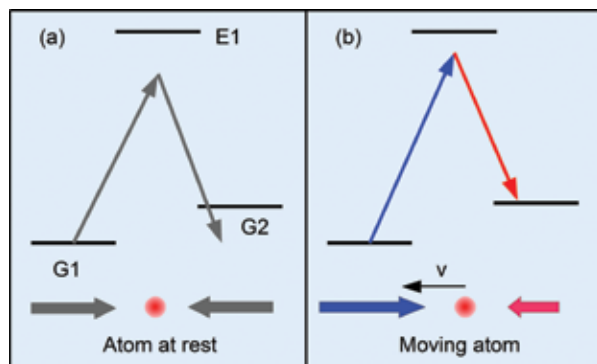
Stimulated Raman Transitions: Velocity selection can occur when atoms are placed in a counterpropagating laser field through stimulated Raman transitions between two ground states, G1 and G2 (see Fig. 9). For an atom at rest, each beam appears to have the same frequency [Fig. 9(a)]. For atoms in motion, however, one beam will be Doppler-shifted to a higher frequency while the other is red-shifted [Fig. 9(b)]. If the apparent frequency difference matches the energy level spacing in the atom, Raman transitions will occur only for that velocity class. In our technique, the two energy levels are magnetic sublevels, which are Zeeman-shifted linearly by a magnetic field. Transitions occur in atoms with Doppler shifts that compensate for the Zeeman shift. Thus, using these two-photon transitions, there is a simple linear relationship between the magnetic field strength and the positions of excited atoms on the camera. The participating energy levels are narrow and capable of discriminating atomic velocities to within 1 mm/s, which corresponds to a magnetic field sensitivity on the order of 1 nT.

Imaging Magnetometry: As an example of the technique, we show background-subtracted images of the expanded atom cloud for different magnetic field strengths. For the images in Fig. 10(a), the fields are spatially uniform. Even without calibration, one can easily use this technique in real time to null magnetic fields simply by zeroing the separation between these stripe features [see the bottom left image of Fig. 10(a)]. If there are spatially varying magnetic fields present, with gradient B' , the resonance condition is also spatially varying and the gradient is intuitively captured in the fluorescence image. For the figures in Fig. 10(b), the atoms were placed in a linear quadrupole field, which occurs at the center of an anti-Helmholtz coil pair. Reference 1 gives a quantitative analysis of this technique.

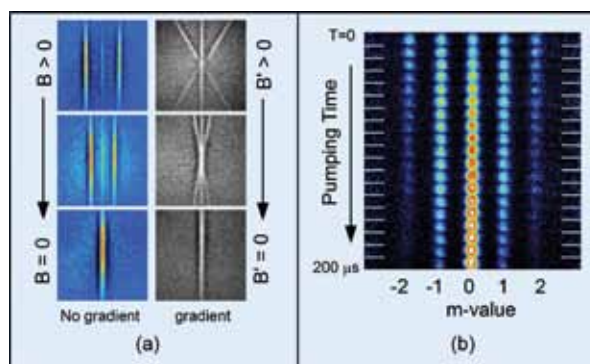
Raman Spectrography: The technique can be slightly modified to measure the population of each magnetic sublevel of a hyperfine manifold simultaneously. By using Raman beams that couple the hyperfine manifolds, which have opposite Zeeman shifts, the selected velocity is also dependent on the magnetic sublevel.² This technique is ideally suited for optimizing optical pumping into a desired sublevel or for measuring sublevel-dependent processes. In Fig. 10(b), we show images of the sublevel distribution as a function of optical pumping pulse duration in a magnetic field. The atoms are in the $F = 2$ hyperfine level, which has $2F + 1$ magnetic sublevels, and are initially equally distributed between $m_F = -2$ to $m_F = 2$, but optical pumping moves the atoms into $m = 0$ in 200 μ s.

**FIGURE 8**

(a) Experiment layout. A cold atom cloud (red circle) is released from a magneto-optical trap and exposed to a retroreflected Raman beam. A CCD camera images the expanding atom cloud from an orthogonal direction, and Helmholtz coils control the magnetic field. (b) Schematic of atom cloud expansion without (left) and with excitation. Resonant velocities (red lines) appear as stripes of increased fluorescence in the image.

**FIGURE 9**

Level diagrams for atoms at rest (a) and in motion (b). The Raman beams are shifted into resonance only for atoms with the correct Doppler shift.

**FIGURE 10**

Background-subtracted fluorescence images of expanding atom clouds after Raman excitation. (a) Magnetometry: The separation between features is directly proportional to the scalar magnetic field (left). Gradient fields, B' , appear as spatially varying resonances (right). (b) Montage of spectrographs of magnetic sublevels for increasing optical pumping pulse durations. The unpolarized sample (top) is pumped into the $m = 0$ state after $200 \mu\text{s}$.

in this example. Reference 2 gives an analysis of this technique.

Summary: We have presented a single-shot technique for imaging magnetic fields over a region with submillimeter spatial resolution using cold atoms. A slight modification allows the technique to measure the populations of several atomic internal states simultaneously. Because the measurements are made in a single shot, they provide useful diagnostics for real-time optimization of cold atom sensors.

[Sponsored by ONR]

References

- ¹ M.L. Terraciano, M. Bashkansky, and F.K. Fatemi, "A Single-shot Imaging Magnetometer Using Cold Atoms," *Opt. Express* **16**, 13062–13069 (2008).
- ² F.K. Fatemi, M.L. Terraciano, M. Bashkansky, and Z. Dutton, "Cold Atom Raman Spectroscopy Using Velocity-selective Resonances," *Opt. Express* **17**, 12971–12980 (2009).